Supporting Information

Dirhenium Core-based Cyclic and Acyclic Helicates as Anticancer Agents towards Breast Cancer and Skin Cancer Cells

Moon Kedia,[a] Sajmina Khatun,[b] Ramar Arumugam,[c] Chandra Lekha Putta,[# b] Bhaskaran Shankar,[#d] Upasana Phukon,[a] Vadapalli Chandrasekhar*[c] Aravind Kumar Rengan*[b] and Malaichamy Sathiyendiran*[a]

[a] School of Chemistry, University of Hyderabad, Hyderabad – 500 046, India.
[b] Department of Biomedical Engineering, Indian Institute of Technology Hyderabad, Kandi – 502 284, India
[c] Department of Chemistry, Tata Institute of Fundamental Research Hyderabad, Hyderabad – 500046, India.
[d] Department of Chemistry, Thiagarajar College of Engineering, Madurai – 625 015, India.

# equal contribution

Contents

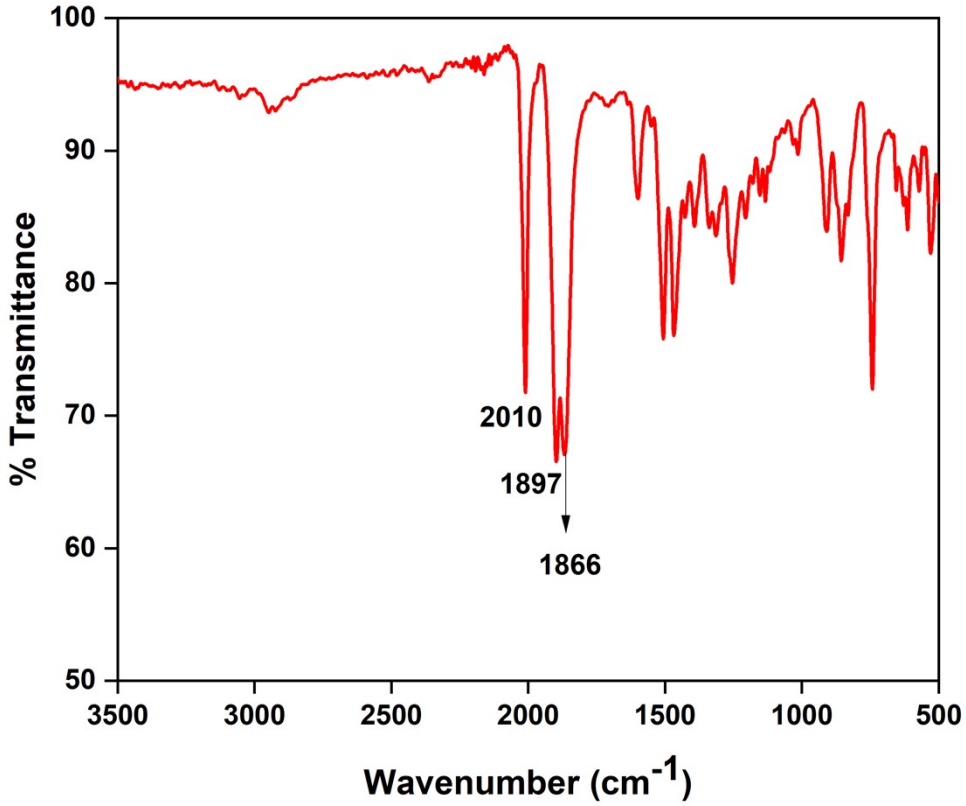

Fig S1. ATR-IR spectrum of **1**.

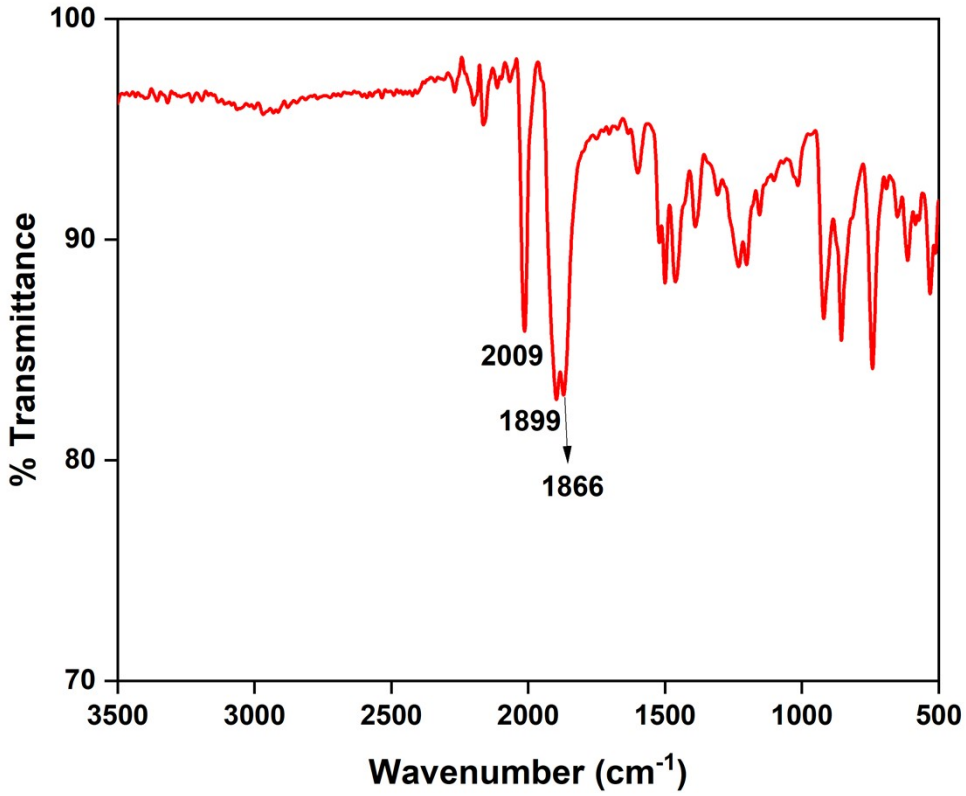

Fig S2. ATR-IR spectrum of **2**.

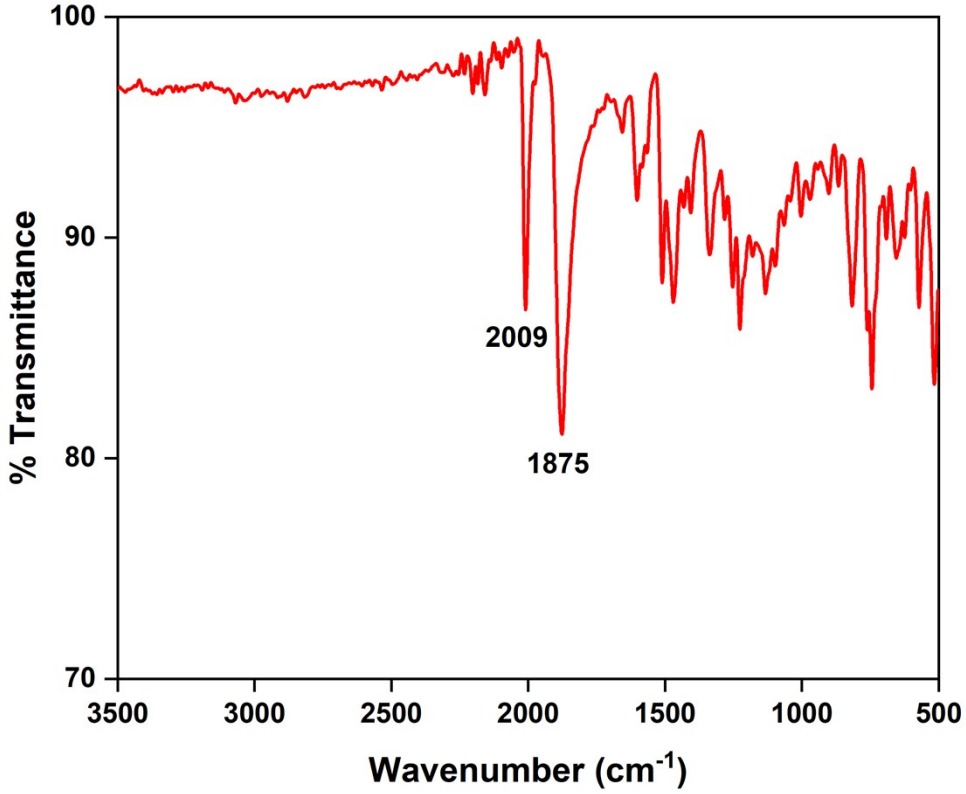

Fig S3. ATR-IR spectrum of **3**.

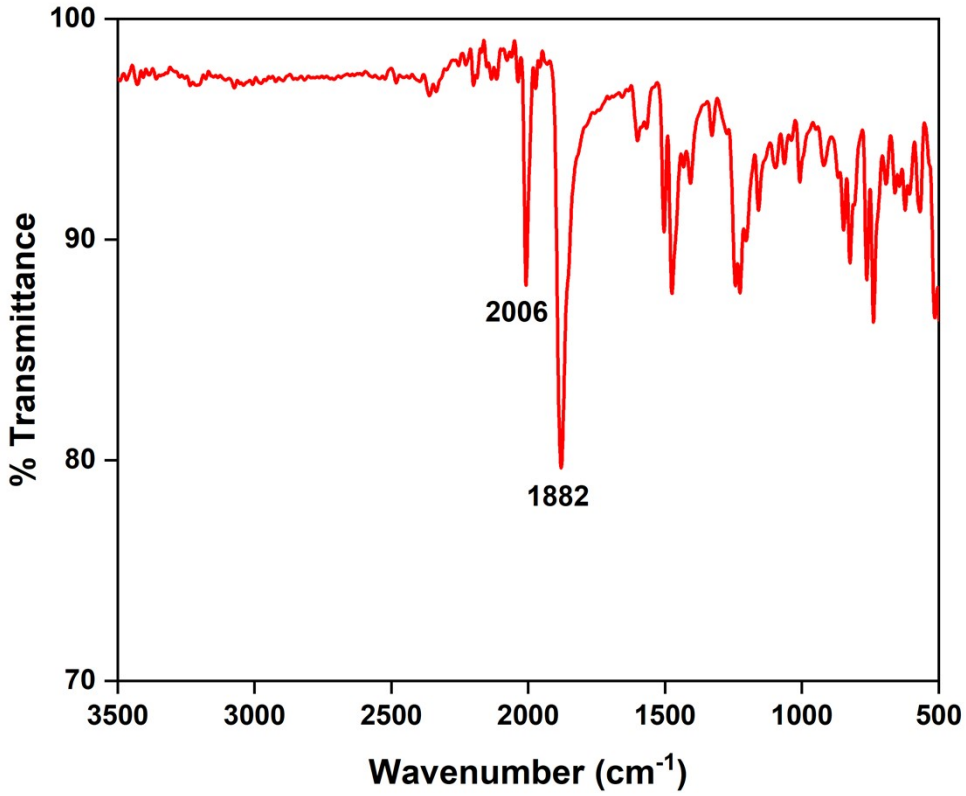

Fig S4. ATR-IR spectrum of **4**.

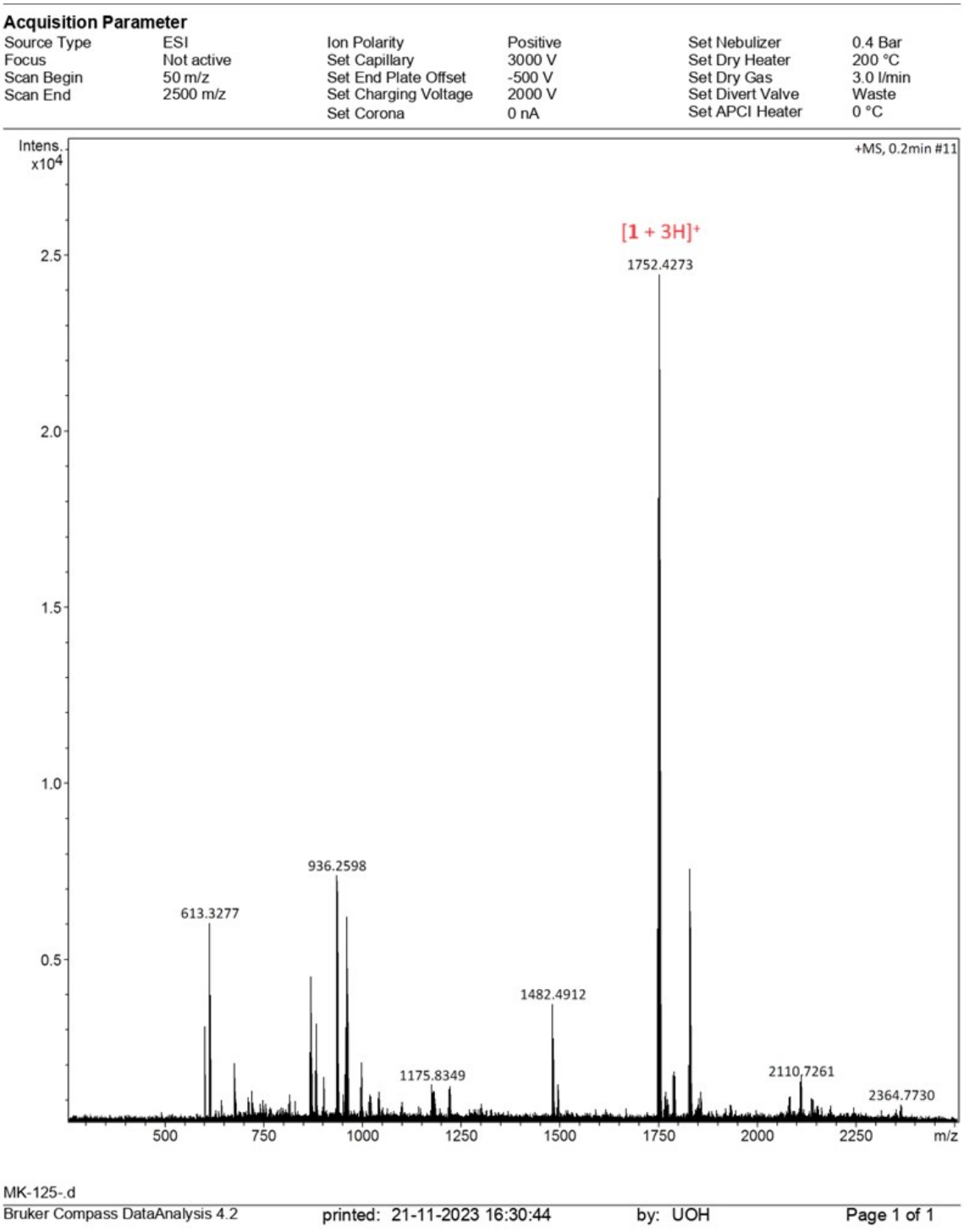

Fig S5. Experimental ESI mass spectrum of [**1** + **3**H]$^+$ in positive ion mode.

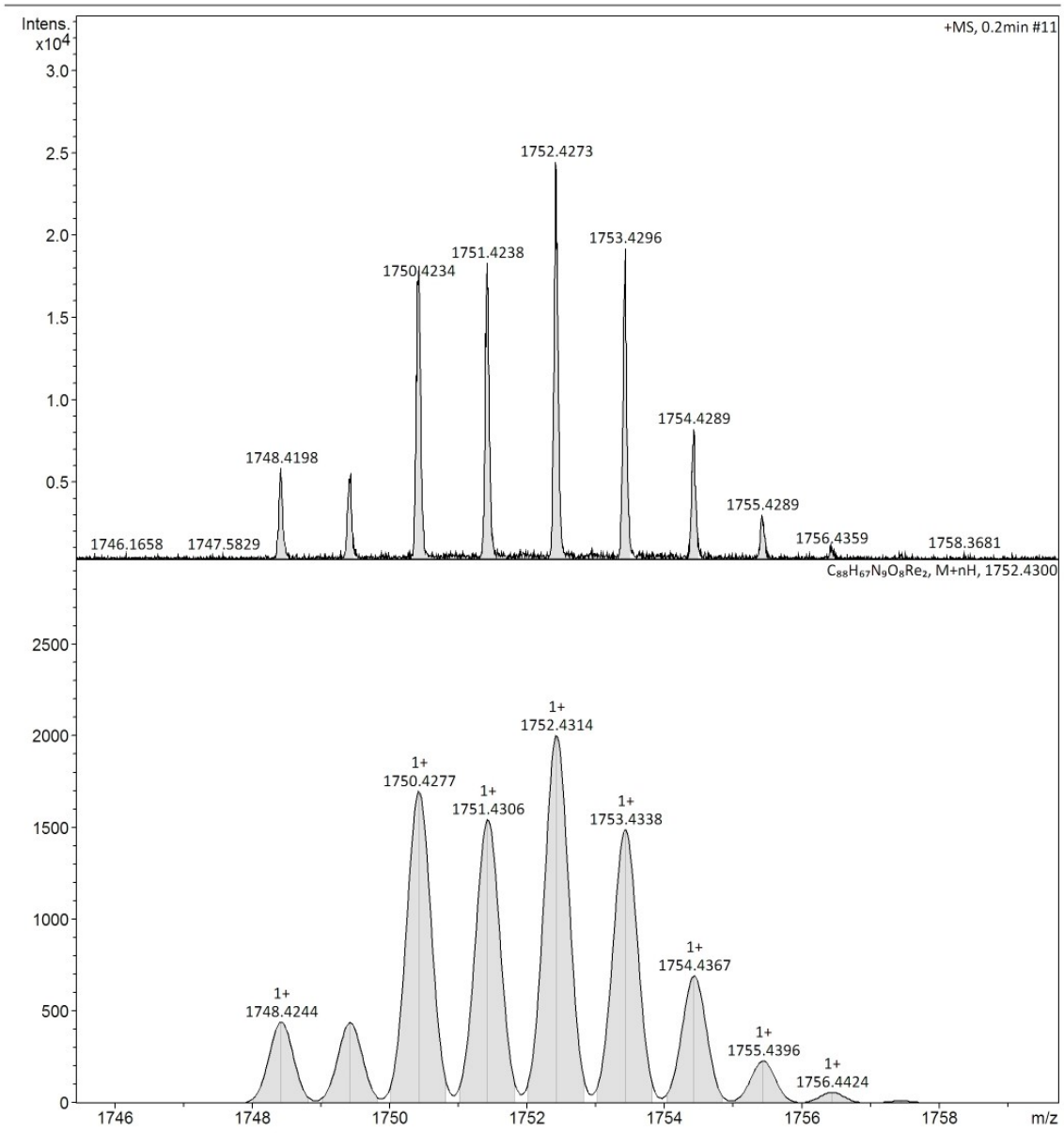

Fig S6. Experimental (Top) and calculated (Bottom) ESI mass spectra of [**1** + 3H]$^+$ in positive ion mode.

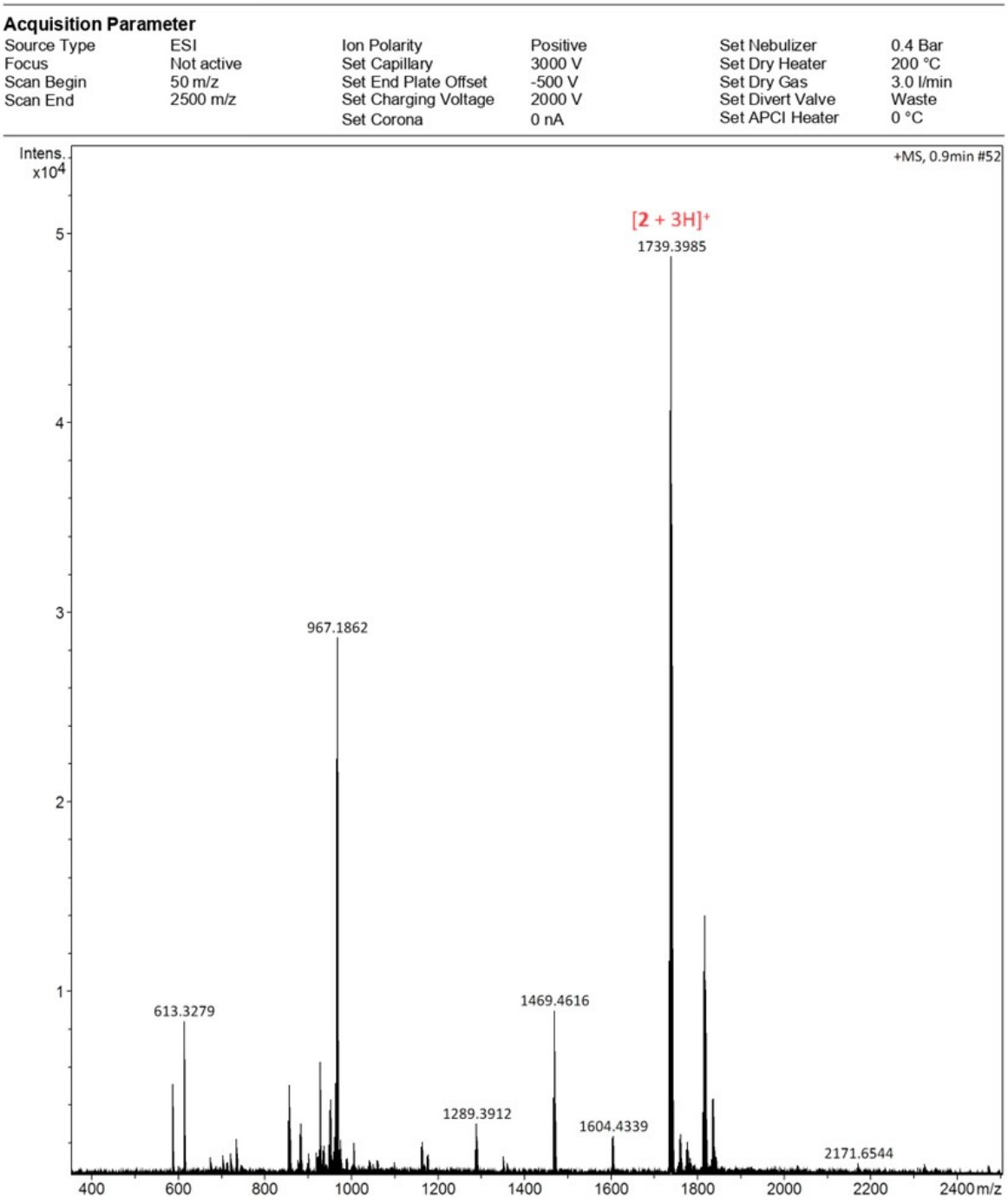

Fig S7. Experimental ESI mass spectrum of [**2** + **3**H]$^+$ in positive ion mode.

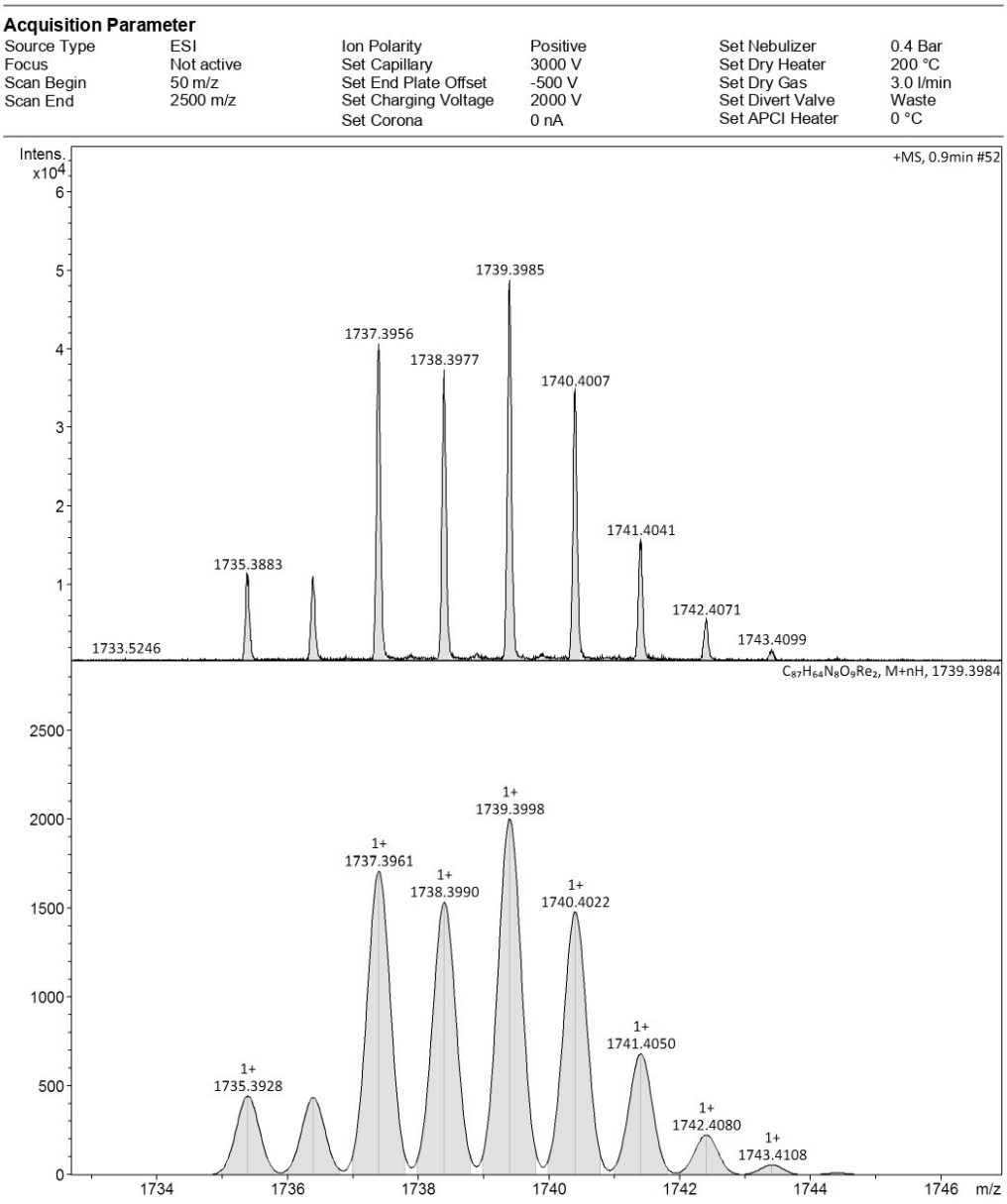

Fig S8. Experimental (Top) and calculated (Bottom) ESI mass spectra of [**2** + 3H]$^+$ in positive ion mode.

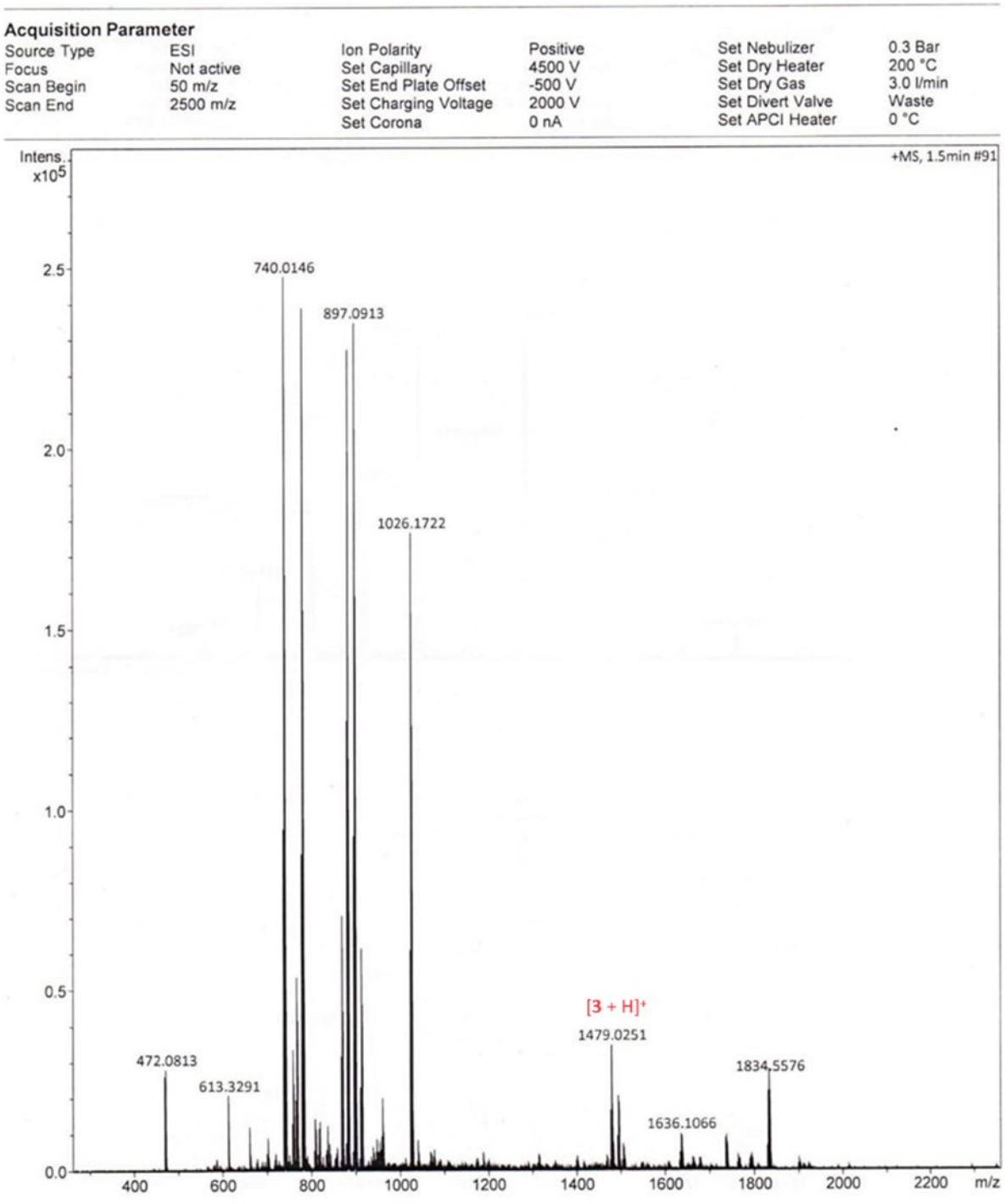

Fig S9. Experimental ESI mass spectrum of [**3** + H]$^+$ in positive ion mode.

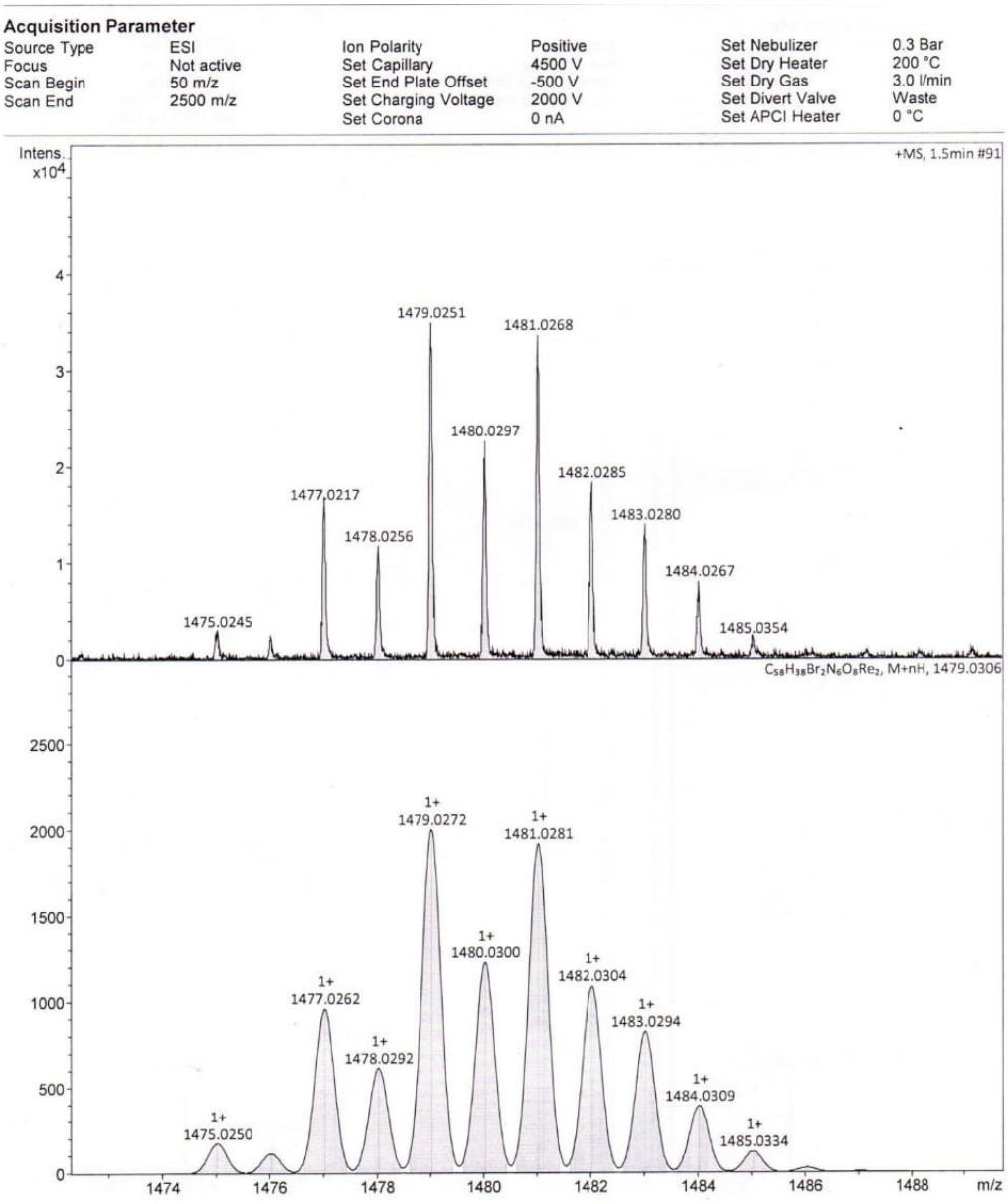

Fig S10. Experimental (Top) and calculated (Bottom) ESI mass spectra of [**3** + H]$^+$ in positive ion mode.

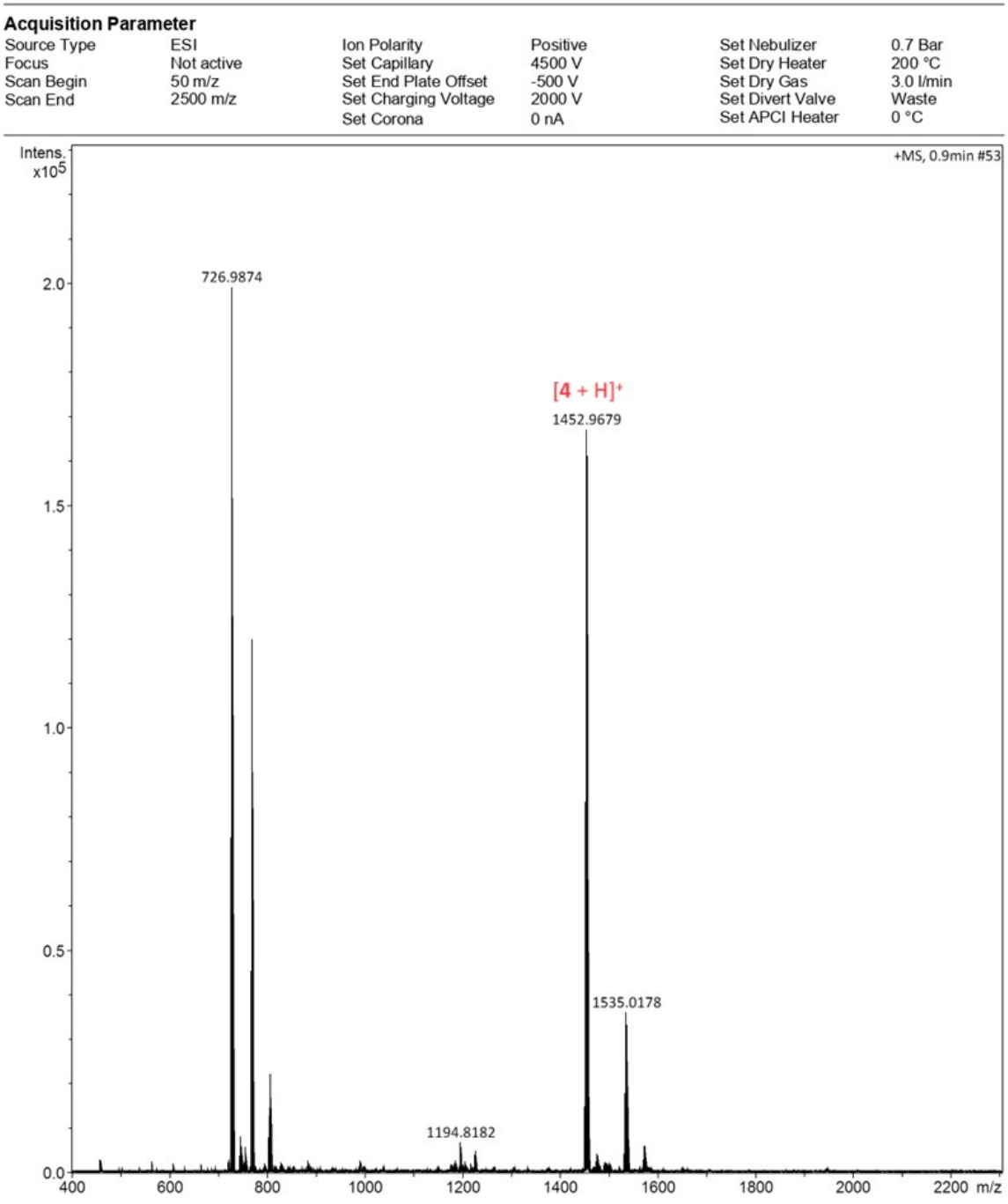

Fig S11. Experimental ESI mass spectrum of [**4** + H]$^+$ in positive ion mode.

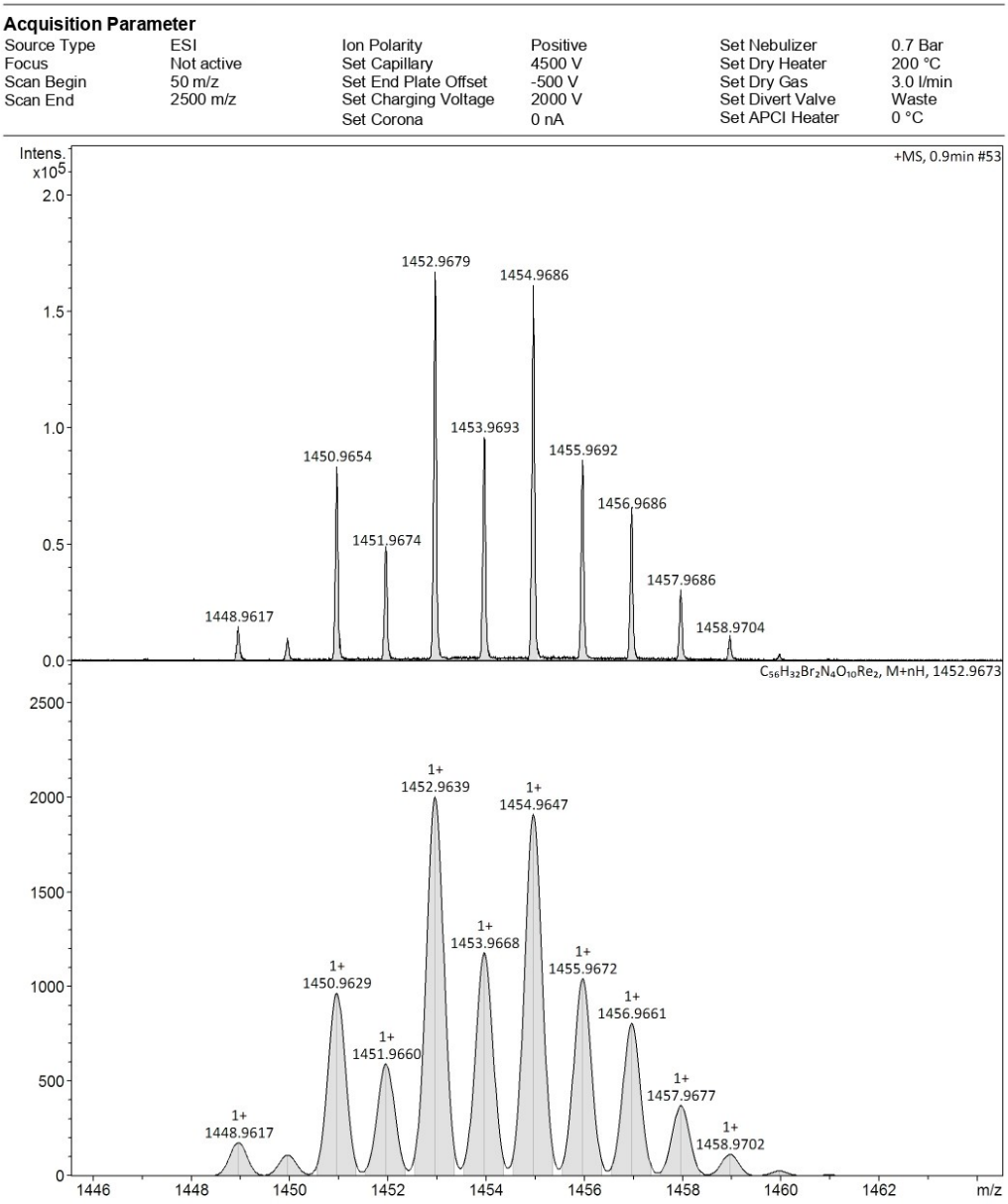

Fig S12. Experimental (Top) and calculated (Bottom) ESI mass spectra of [**4** + H]$^+$ in positive ion mode.

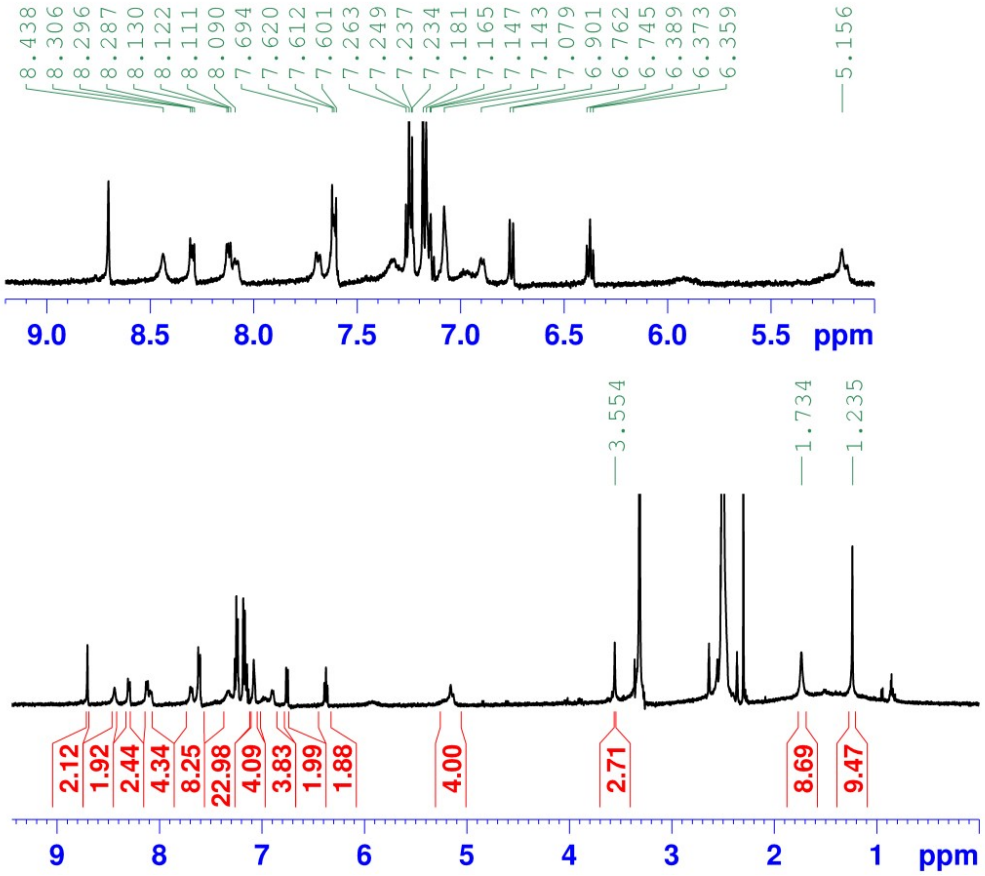

Fig S13. ^{1}H-NMR spectrum of **1** in DMSO-d_6.

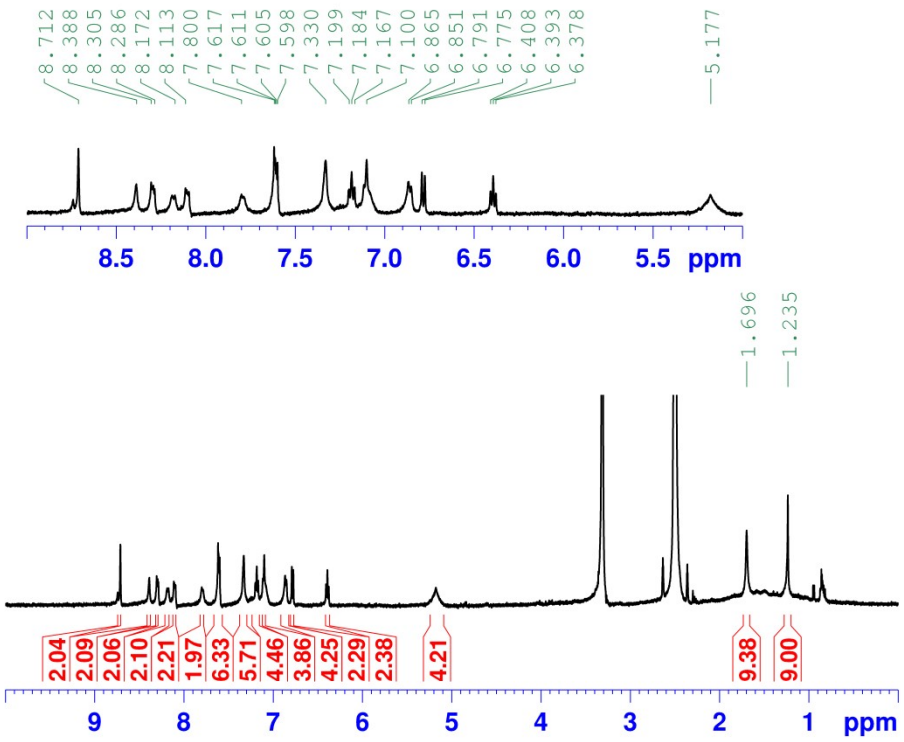

Fig S14. ^{1}H-NMR spectrum of **2** in DMSO-d_6.

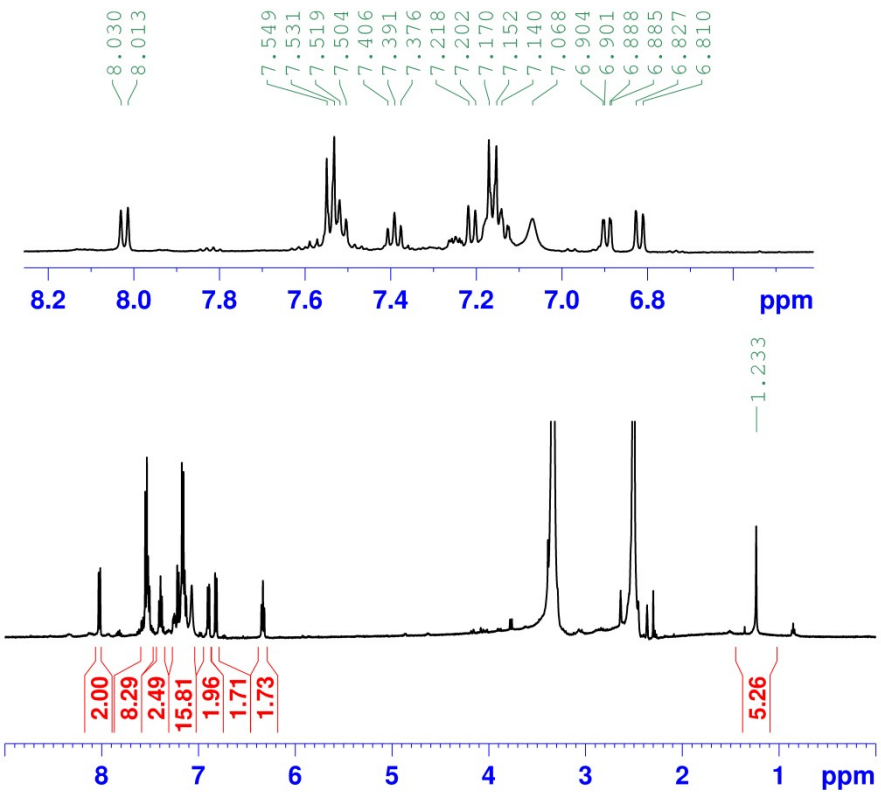

Fig S15. ^{1}H-NMR spectrum of **3** in DMSO-d_6.

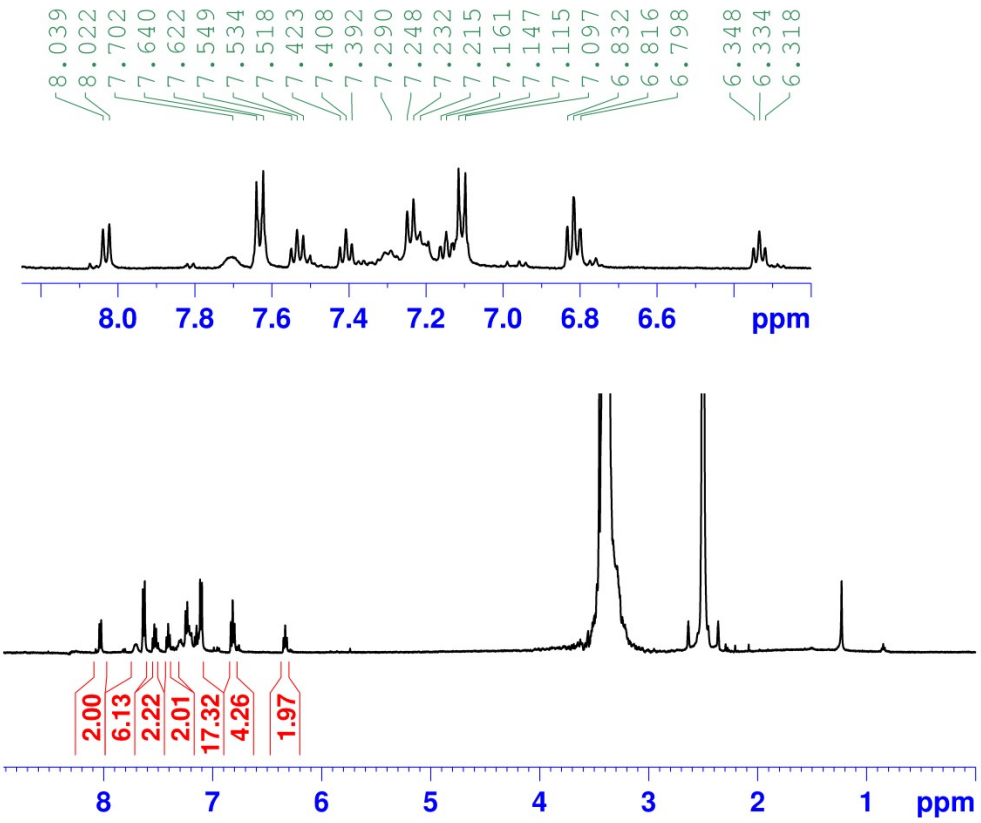

Fig S16. ^{1}H-NMR spectrum of **4** in DMSO-d_6.

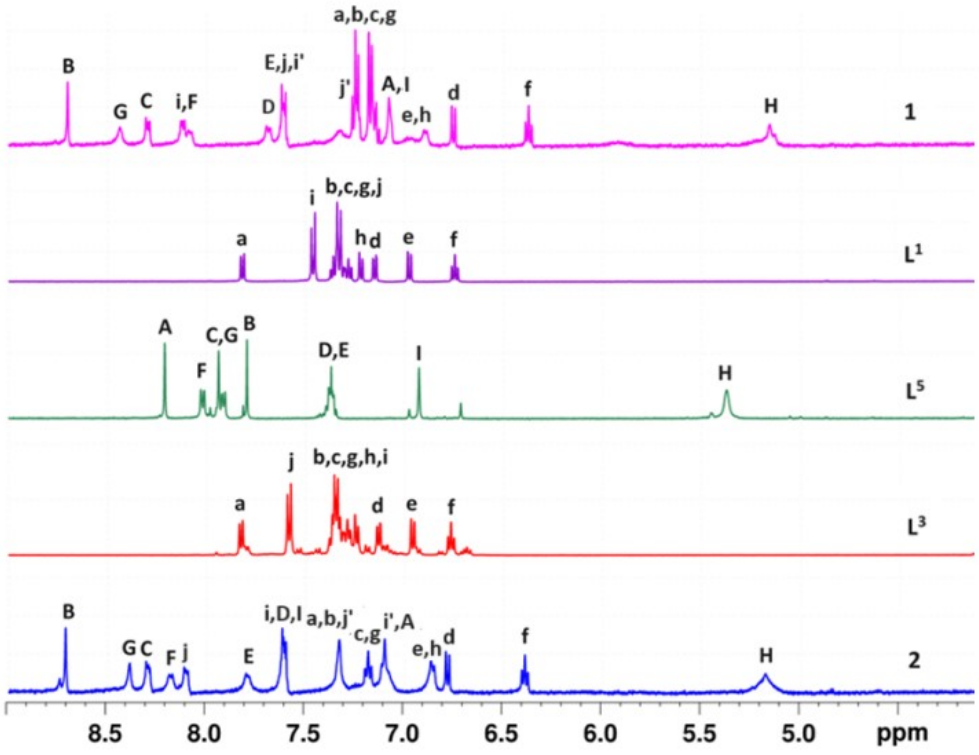

Fig S17. Partial ^{1}H NMR spectra of **1** and **2** with the corresponding ligands in DMSO-d_6 at 298 K.

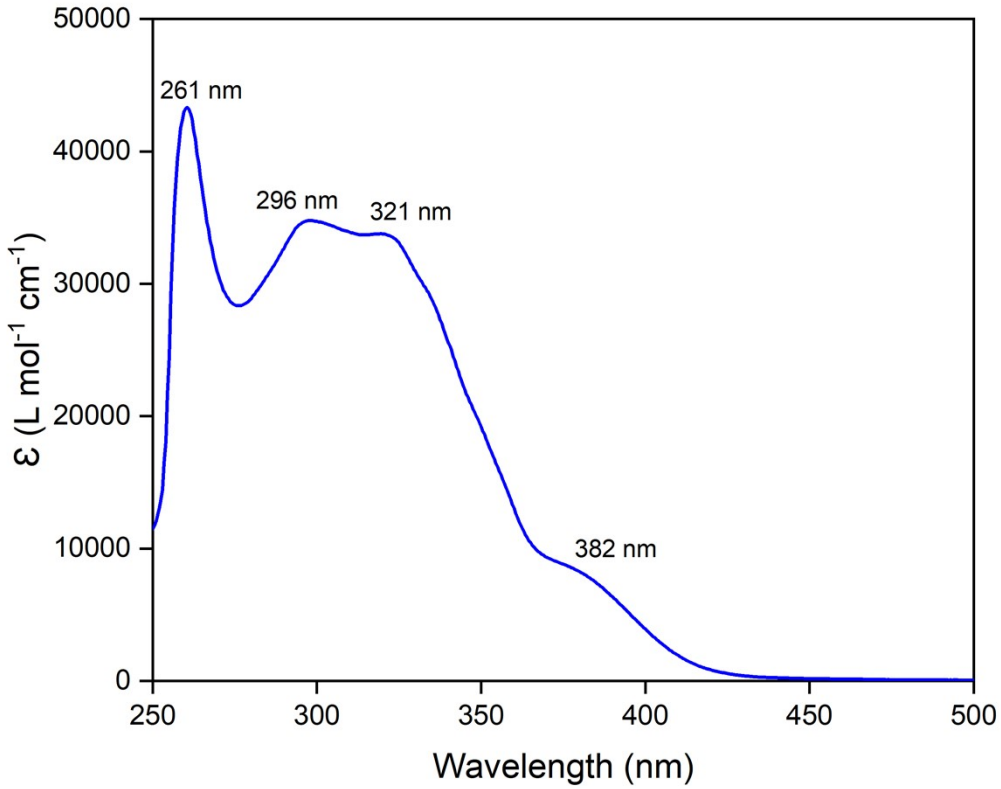

Fig S18. UV-visible absorption spectra of **1** in DMSO at room temperature

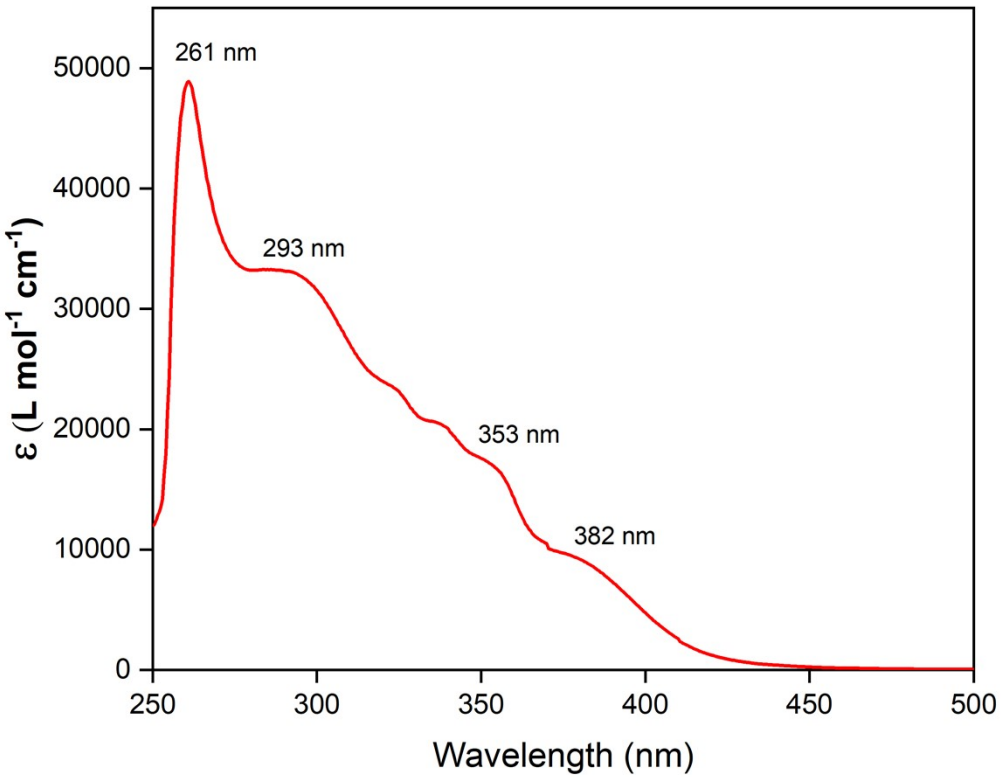

Fig S19. UV-visible absorption spectra of **2** in DMSO at room temperature

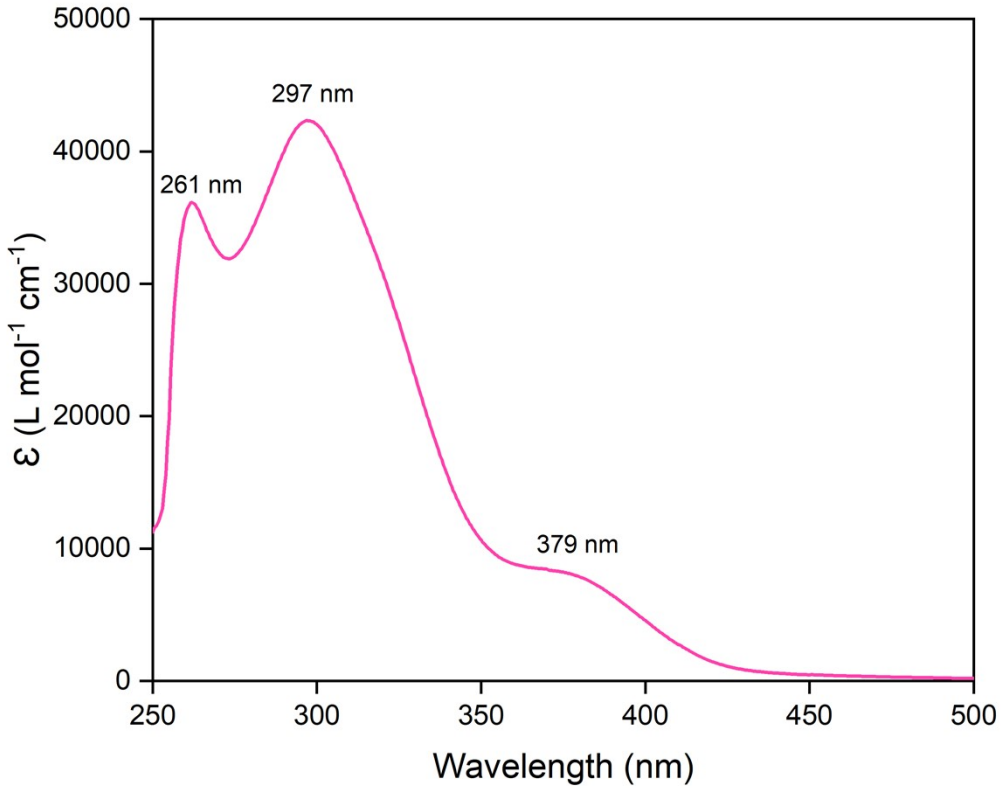

Fig S20. UV-visible absorption spectra of **3** in DMSO at room temperature

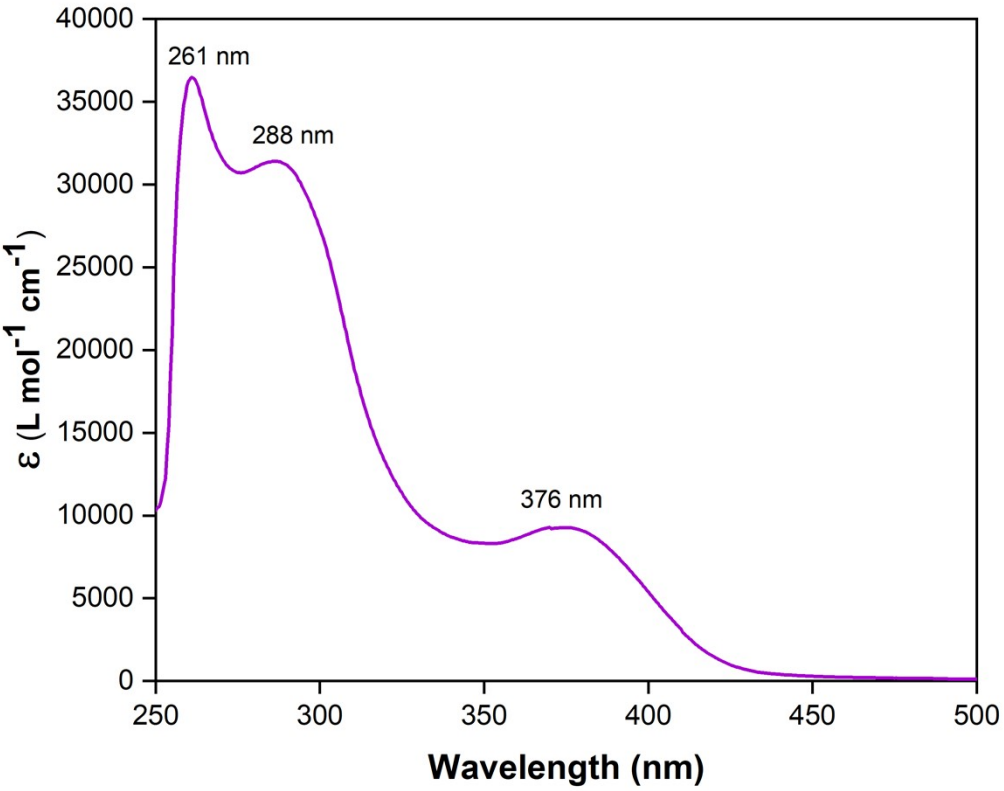

Fig S21. UV-visible absorption spectra of **4** in DMSO at room temperature

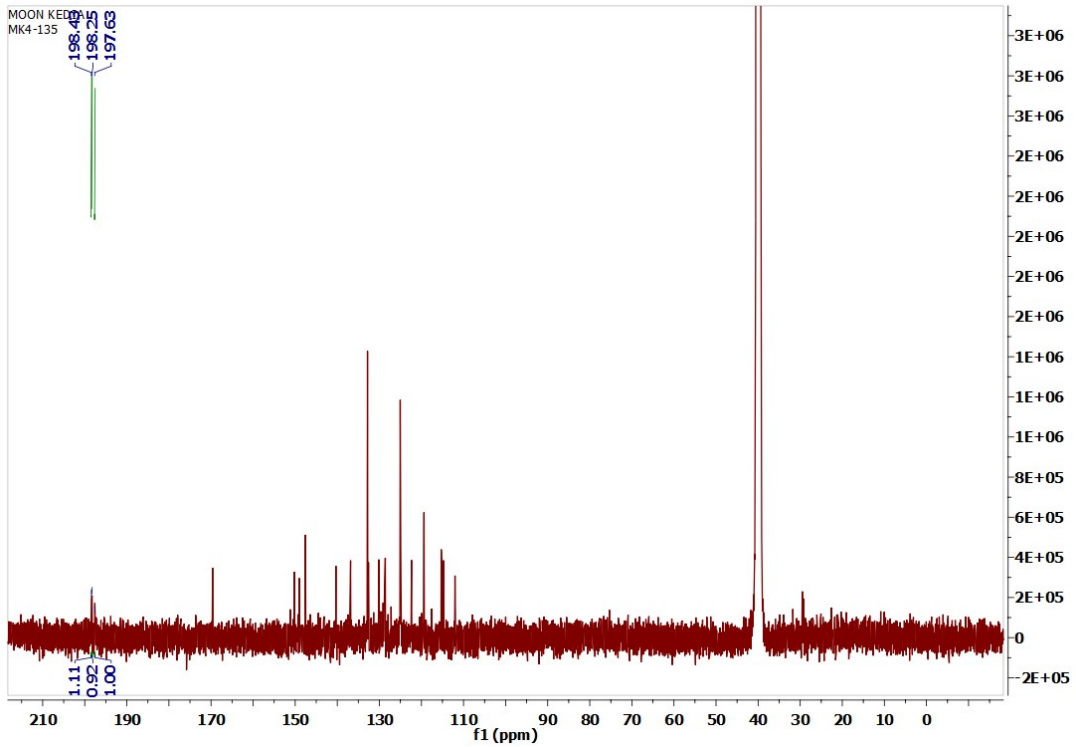

Fig S22. ^{13}C-NMR spectrum of **3** in DMSO-d_6.

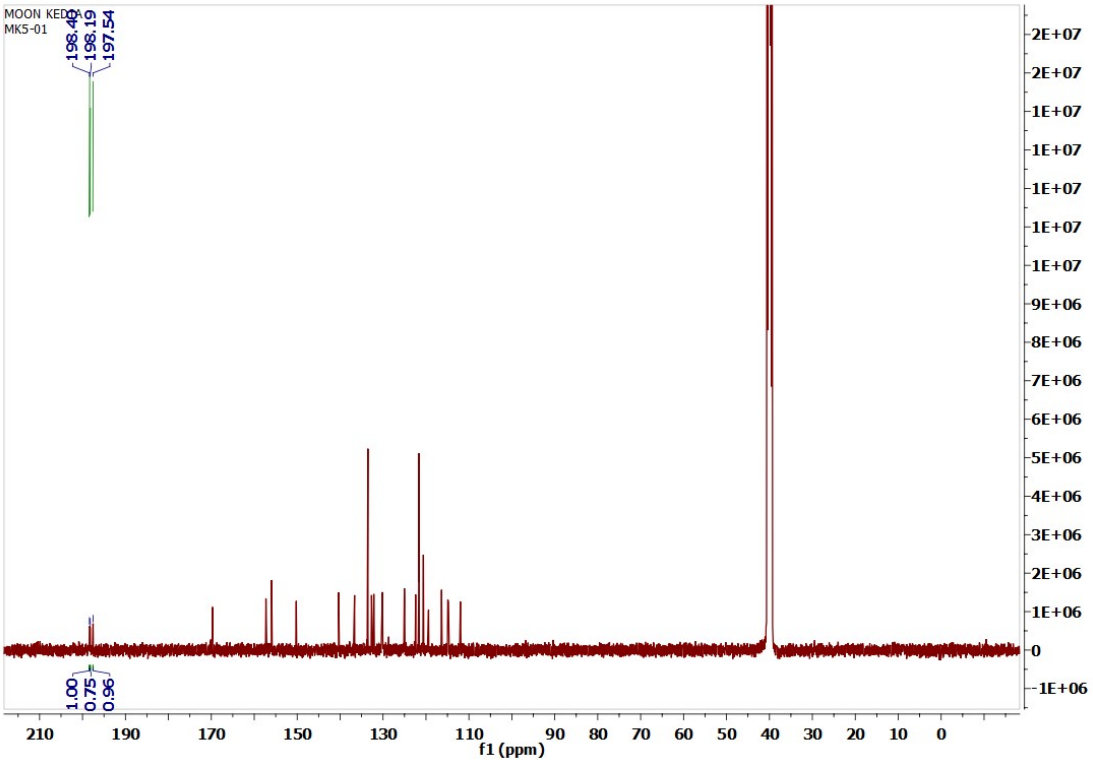

Fig S23. ^{13}C-NMR spectrum of **4** in DMSO-d_6.

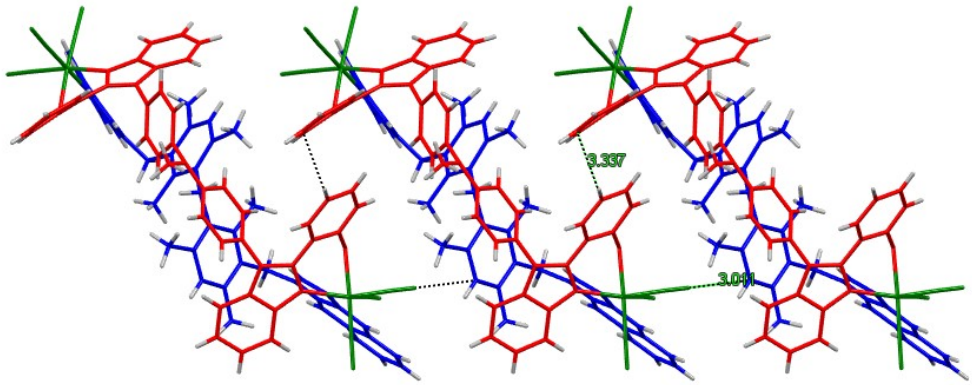

Fig S24. Crystal structure of **1** displaying the intermolecular interactions.

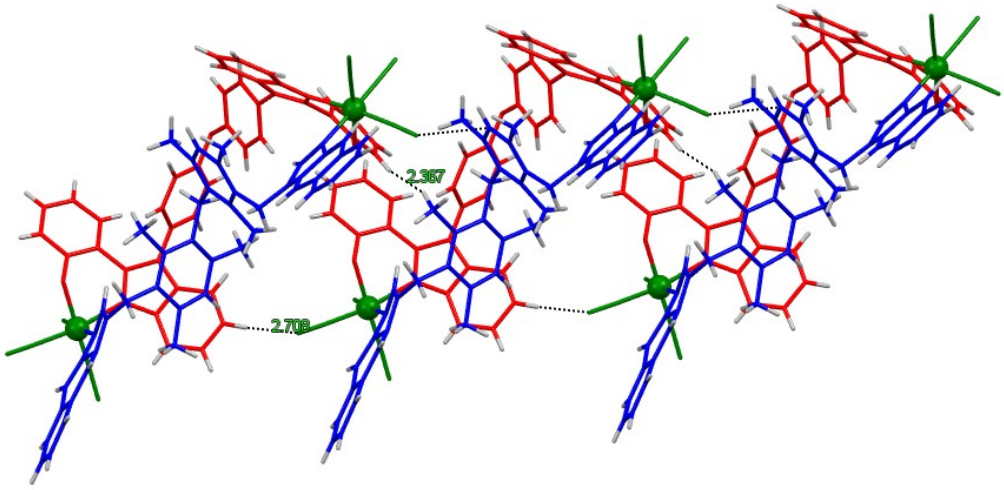

Fig S25. Crystal structure of **2** displaying the intermolecular interactions.

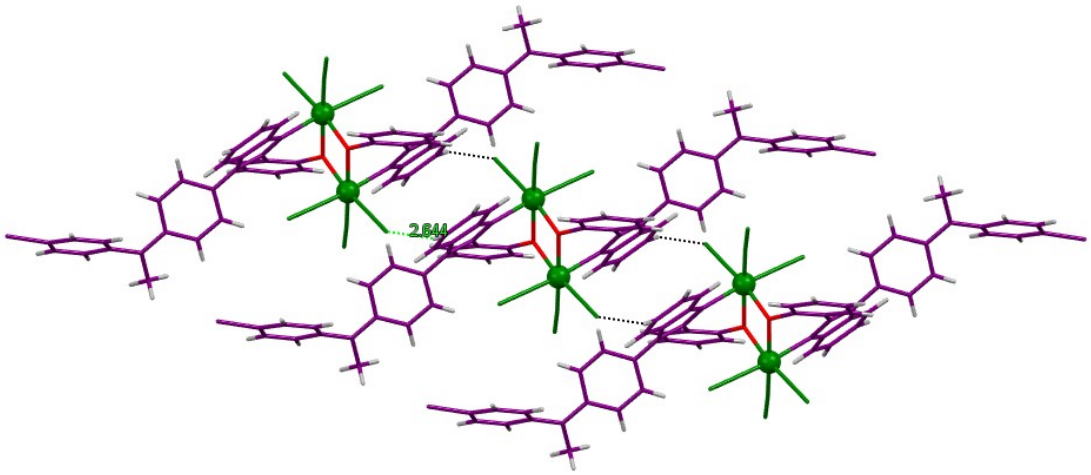

Fig S26. Crystal structure of **3** displaying the intermolecular interactions.

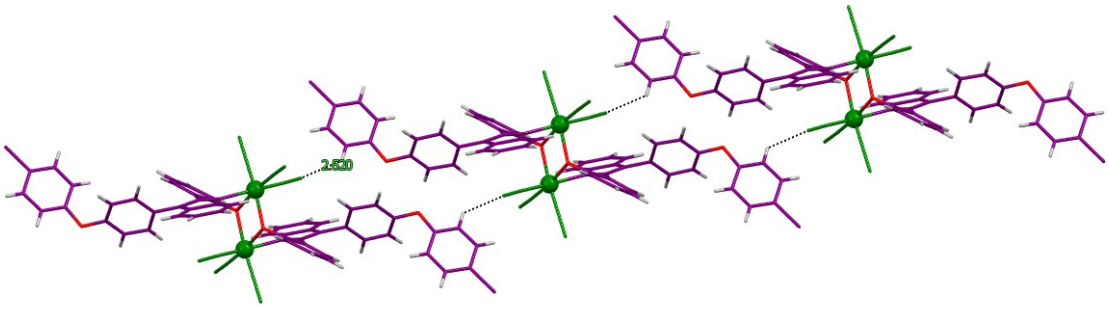

Fig S27. Crystal structure of **4** displaying the intermolecular interactions.

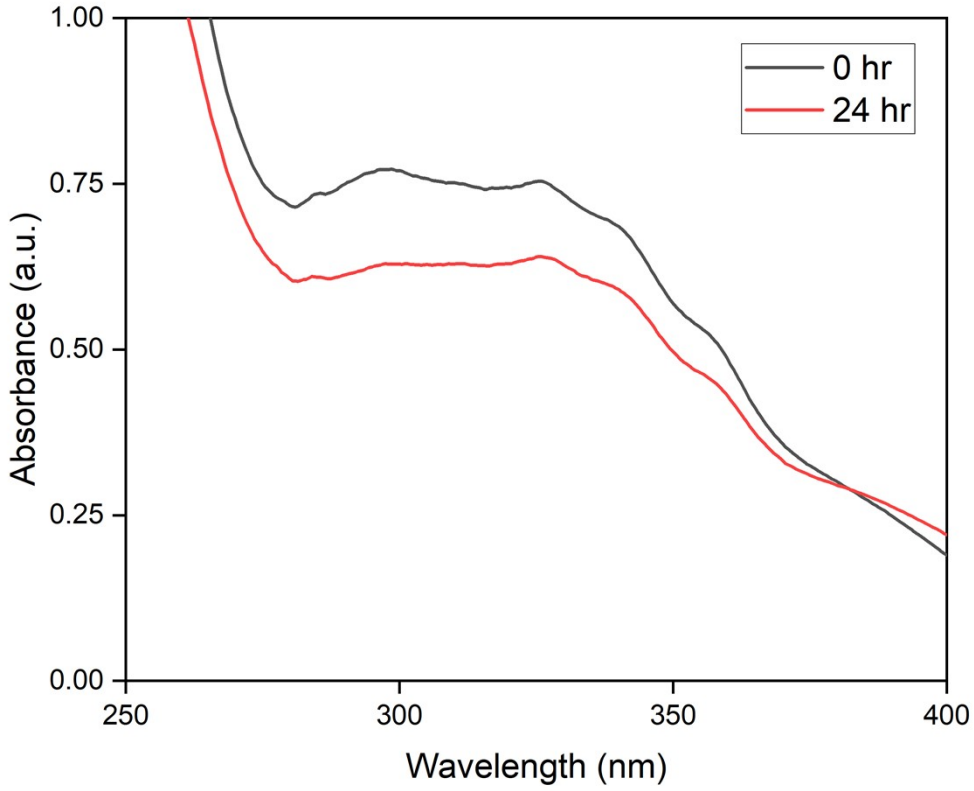

Fig S28. UV-visible absorption spectra of **1** in 0.1 % DMSO/RPMI for 24 hr at room temperature.

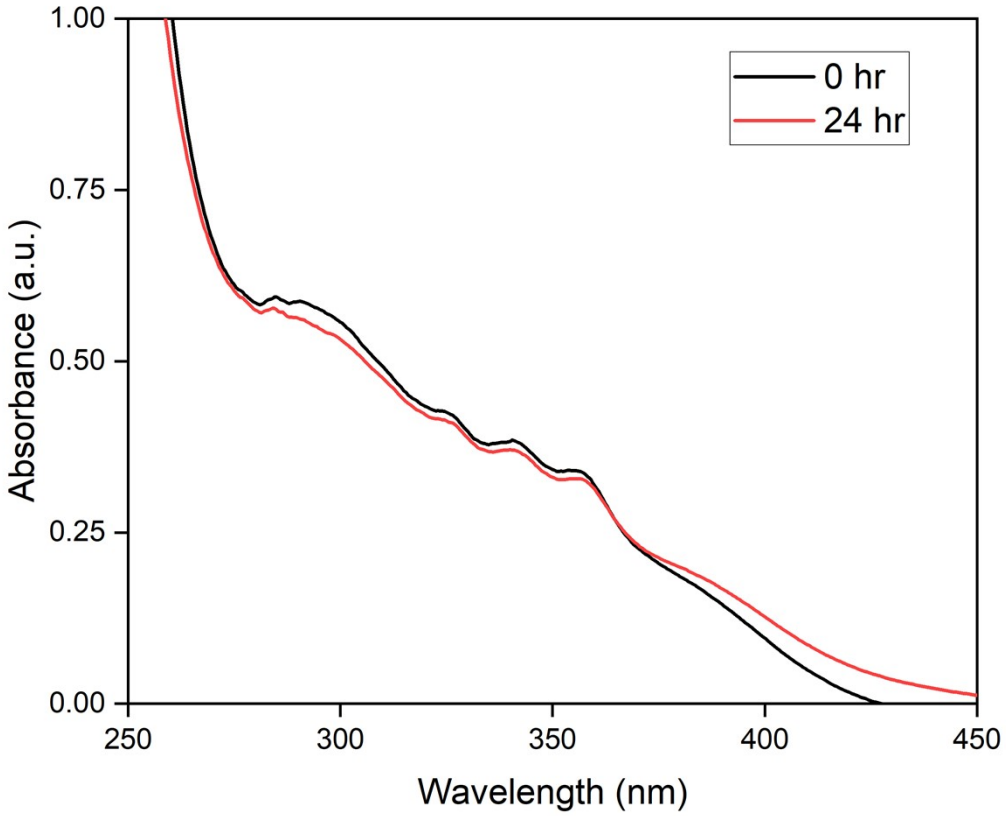

Fig S29. UV-visible absorption spectra of **2** in 0.1 % DMSO/RPMI for 24 hr at room temperature.

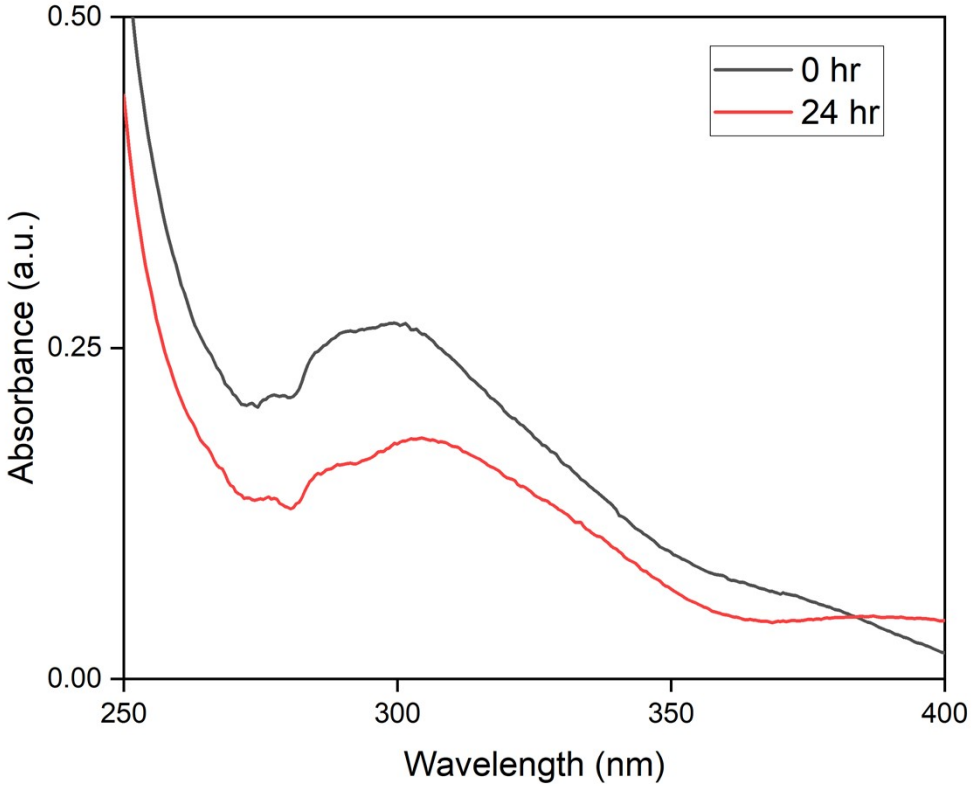

Fig S30. UV-visible absorption spectra of **3** in 0.1 % DMSO/RPMI for 24 hr at room temperature.

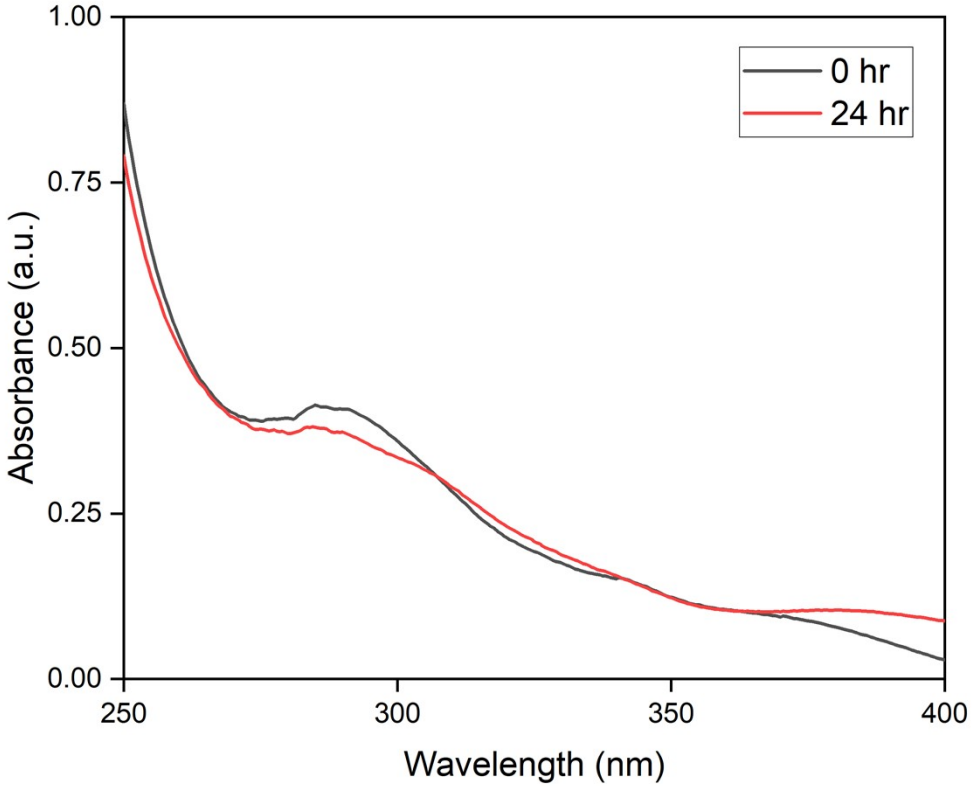

Fig S31. UV-visible absorption spectra of **4** in 0.1 % DMSO/RPMI for 24 hr at room temperature.

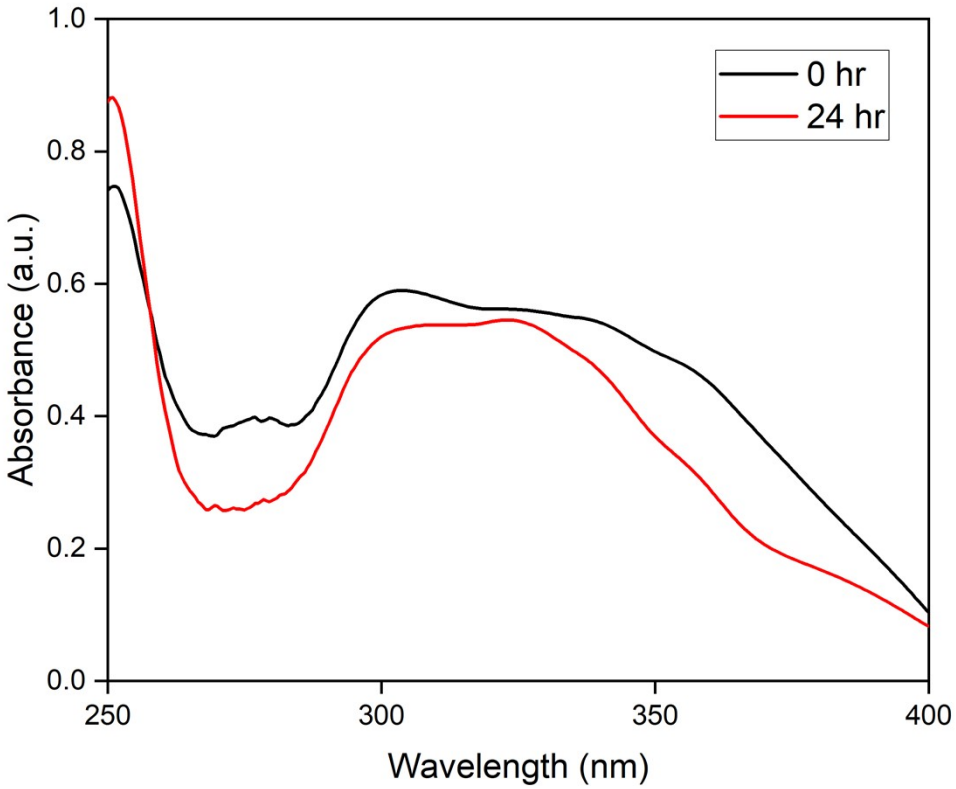

Fig S32. UV-visible absorption spectra of **1** in 0.1 % DMSO/DMEM for 24 hr at room temperature.

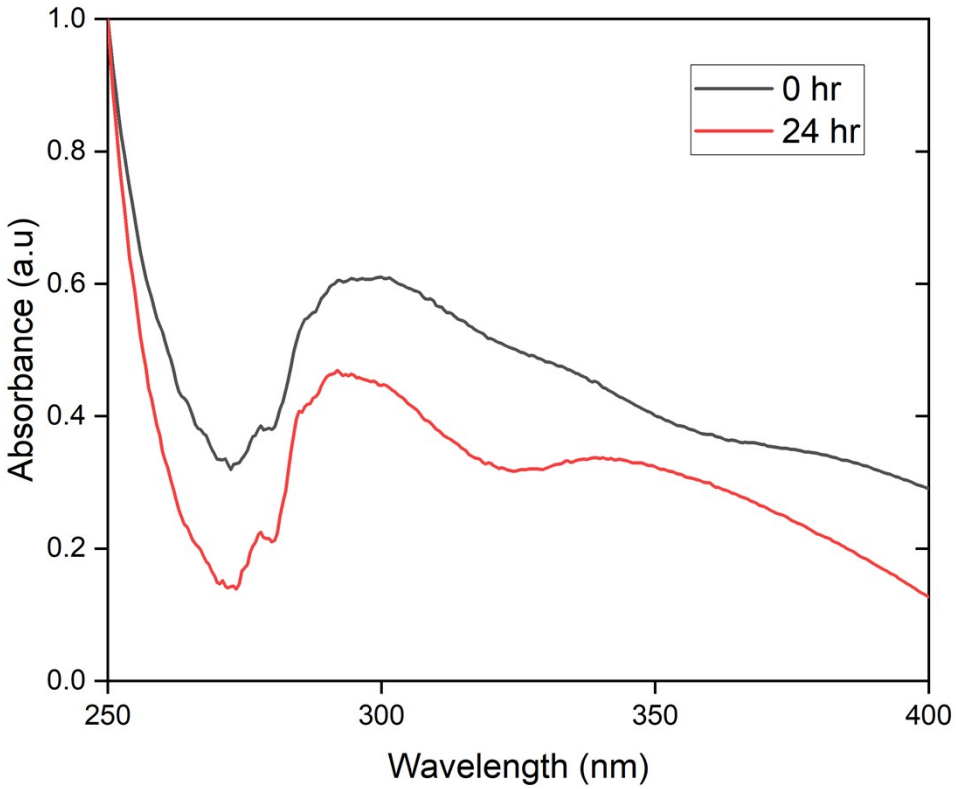

Fig S33. UV-visible absorption spectra of **3** in 0.1 % DMSO/DMEM for 24 hr at room temperature.

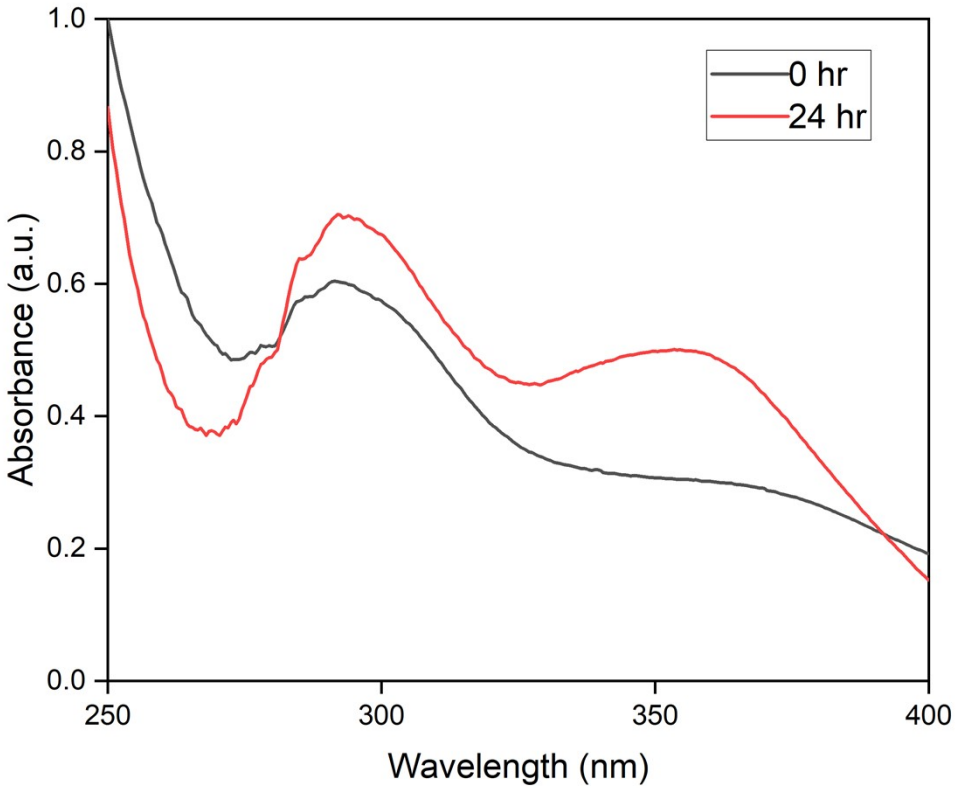

Fig S34. UV-visible absorption spectra of **4** in 0.1 % DMSO/DMEM for 24 hr at room temperature.

Element	Weight%
C	64.20
N	6.89
O	18.18

Table S1. Elemental Composition of **1**.

Element	Weight%
C	65.63
N	5.04
O	17.58

Table S2. Elemental Composition of **2**.

Element	Weight%
C	54.42
N	6.23
O	18.59

Table S3. Elemental Composition of **3**.

Element	Weight%
C	52.96
N	4.76
O	13.00

Table S4. Elemental Composition of **4**.

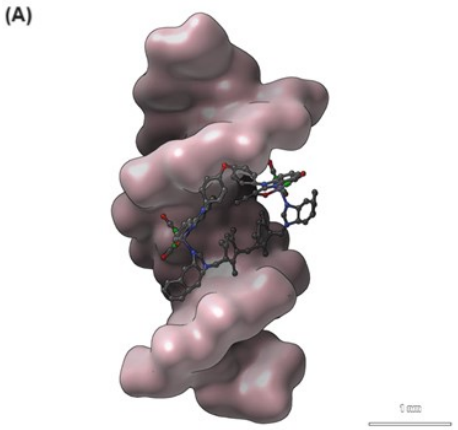

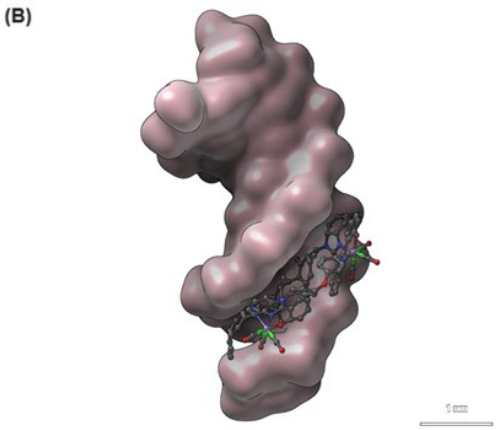

(C)

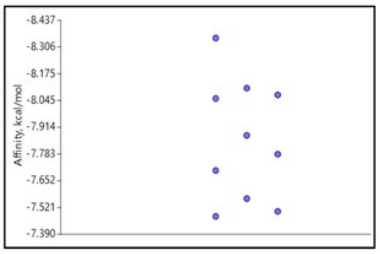

(D)

Docking Site	Mean Binding Affinity (kcal/mol)	Number of poses
Minor Groove	-8.173 ± 0.154	3
Major Groove	-7.706 ± 0.210	7
Overall DNA Helix	**-7.846 ± 0.293**	**10**

Fig S35: Docking of Complex **2** with a B-DNA fragment. (A-B) Rendered images of **2** docked in the major and minor grooves of B-DNA fragment, respectively. (C) Scatter plot of binding affinities of **2** with B-DNA fragment in various poses. (D) Mean binding affinity of **2** with B-DNA fragment.

Identification code	MS183	
Empirical formula	C88 H67 N9 O8 Re2	
Formula weight	1750.90	
Temperature	296(2) K	
Wavelength	0.71073 Å	
Crystal system	Triclinic	
Space group	P -1	
Unit cell dimensions	a = 11.907(4) Å	□= 95.328(12)°.
	b = 15.980(5) Å	□= 99.706(12)°.
	c = 21.286(7) Å	□ = 108.576(11)°.
Volume	3737(2) $Å^3$	
Z	2	
Density (calculated)	1.556 Mg/m^3	
Absorption coefficient	3.301 mm^{-1}	
F(000)	1744	
Crystal size	0.120 x 0.100 x 0.080 mm^3	
Theta range for data collection	1.549 to 25.000°.	
Index ranges	-14<=h<=14, -18<=k<=18, -25<=l<=25	
Reflections collected	122183	
Independent reflections	13148 [R(int) = 0.0896]	
Completeness to theta = 25.000°	99.9 %	
Absorption correction	Semi-empirical from equivalents	
Max. and min. transmission	0.778 and 0.693	
Refinement method	Full-matrix least-squares on F^2	
Data / restraints / parameters	13148 / 235 / 1027	
Goodness-of-fit on F^2	1.065	
Final R indices [I>2sigma(I)]	R1 = 0.0471, wR2 = 0.1024	
R indices (all data)	R1 = 0.0720, wR2 = 0.1119	
Extinction coefficient	n/a	
Largest diff. peak and hole	1.763 and -0.860 $e.Å^{-3}$	

Table S5. Crystal data and structure refinement for **1**.

Identification code	MS180sq	
Empirical formula	C87 H64 N8 O9 Re2	
Formula weight	1737.86	
Temperature	296(2) K	
Wavelength	0.71073 Å	
Crystal system	Triclinic	
Space group	P -1	
Unit cell dimensions	a = 11.868(3) Å	□= 73.724(10)°.
	b = 16.021(5) Å	□= 81.450(10)°.
	c = 24.569(7) Å	□ = 81.869(10)°.
Volume	4410(2) $Å^3$	
Z	2	
Density (calculated)	1.309 Mg/m^3	
Absorption coefficient	2.798 mm^{-1}	
F(000)	1728	
Crystal size	0.120 x 0.100 x 0.080 mm^3	
Theta range for data collection	1.745 to 27.605°.	
Index ranges	-15<=h<=15, -20<=k<=20, -31<=l<=31	
Reflections collected	178132	
Independent reflections	20284 [R(int) = 0.0913]	
Completeness to theta = 25.242°	99.7 %	
Absorption correction	Semi-empirical from equivalents	
Refinement method	Full-matrix least-squares on F^2	
Data / restraints / parameters	20284 / 3844 / 1364	
Goodness-of-fit on F^2	1.021	
Final R indices [I>2sigma(I)]	R1 = 0.0460, wR2 = 0.1077	
R indices (all data)	R1 = 0.0799, wR2 = 0.1174	
Extinction coefficient	n/a	
Largest diff. peak and hole	2.350 and -0.754 $e.Å^{-3}$	

Table S6. Crystal data and structure refinement for **2**.

Identification code	MS327	
Empirical formula	C58 H38 Br2 N6 O8 Re2	
Formula weight	1479.16	
Temperature	296(2) K	
Wavelength	0.71073 Å	
Crystal system	Triclinic	
Space group	P -1	
Unit cell dimensions	a = 8.8344(3) Å	□= 77.077(3)°.
	b = 10.7537(5) Å	□= 84.333(3)°.
	c = 14.2997(5) Å	□ = 80.686(3)°.
Volume	1303.88(9) $Å^3$	
Z	1	
Density (calculated)	1.884 Mg/m^3	
Absorption coefficient	6.233 mm^{-1}	
F(000)	712	
Crystal size	0.100 x 0.080 x 0.080 mm^3	
Theta range for data collection	1.963 to 24.997°.	
Index ranges	-10<=h<=10, -12<=k<=12, -17<=l<=16	
Reflections collected	28078	
Independent reflections	4588 [R(int) = 0.0982]	
Completeness to theta = 24.997°	100.0 %	
Absorption correction	Semi-empirical from equivalents	
Max. and min. transmission	1.00000 and 0.09847	
Refinement method	Full-matrix least-squares on F^2	
Data / restraints / parameters	4588 / 0 / 344	
Goodness-of-fit on F^2	1.039	
Final R indices [I>2sigma(I)]	R1 = 0.0523, wR2 = 0.1317	
R indices (all data)	R1 = 0.0623, wR2 = 0.1368	
Extinction coefficient	n/a	
Largest diff. peak and hole	2.440 and -1.683 $e.Å^{-3}$	

Table S7. Crystal data and structure refinement for **3**.

Identification code	MS332	
Empirical formula	C56 H32 Br2 N4 O10 Re2	
Formula weight	1453.07	
Temperature	296(2) K	
Wavelength	0.71073 Å	
Crystal system	Monoclinic	
Space group	P 21/n	
Unit cell dimensions	a = 8.9344(2) Å	□= 90°.
	b = 16.4337(4) Å	□= 91.369(2)°.
	c = 17.0034(4) Å	□ = 90°.
Volume	2495.82(10) $Å^3$	
Z	2	
Density (calculated)	1.934 Mg/m^3	
Absorption coefficient	6.512 mm^{-1}	
F(000)	1392	
Crystal size	0.100 x 0.080 x 0.080 mm^3	
Theta range for data collection	2.396 to 24.998°.	
Index ranges	-10<=h<=10, -18<=k<=19, -20<=l<=20	
Reflections collected	22693	
Independent reflections	4387 [R(int) = 0.0584]	
Completeness to theta = 24.998°	99.7 %	
Absorption correction	Semi-empirical from equivalents	
Max. and min. transmission	1.00000 and 0.04881	
Refinement method	Full-matrix least-squares on F^2	
Data / restraints / parameters	4387 / 0 / 334	
Goodness-of-fit on F^2	1.072	
Final R indices [I>2sigma(I)]	R1 = 0.0401, wR2 = 0.1157	
R indices (all data)	R1 = 0.0494, wR2 = 0.1195	
Extinction coefficient	n/a	
Largest diff. peak and hole	2.294 and -1.417 $e.Å^{-3}$	

Table S8. Crystal data and structure refinement for **4**.

Complex	Intermolecular Interaction	Distance	Angle
1	(a) hydrogen bonding, $-CH_3$ (mesityl spacer)···O (O≡C–Re) (b) C–H···π interaction between benzimidazolyl proton of L^1 and naphthanoimidazolyl motif of L^5. (c) C–H···π interaction between methyl proton (N–Me) of L^1 of one molecule and the phenyl motif of L^1 of another. (d) C–H···π interaction (d = 2.83 Å; θ = ~142°).	(a) 2.52 Å (b) 2.88 Å (c) 2.68 Å	(a) 136° (b) 158° (c) 152°
2	(a) C–H···π interaction between mesityl $-CH_3$ proton of L^5 of one molecule to naphthanoimidazolyl motif of L^5 of the adjacent molecule (b) hydrogen bond C–H (aromatic)···O (L^3) (c) hydrogen bonding, C–H (aromatic)···O (O≡C–Re) (d) C–H···π interaction	(a) 2.89 Å (b) 2.39 Å (c) 2.57 Å (d) 2.83 Å	(a) 121° (b) 145° (c) 127° (d) 142°
3	(a) C–H (aromatic)···O (O≡C–Re)	(a) 2.64 Å	(a) 153°
4	(a) H–Br bonding (b) C–H (aromatic)···O (O≡C–Re)	(a) 3.04 Å (b) 2.67Å	(a) 133° (b) 135°

Table S9. Intermolecular Interactions present in **1**-**4**.